

Water vapour transport through perforated foils

Wim van der Spoel

TU Delft, Faculty of Civil Engineering and Geosciences, Section Building Engineering,

Stevinweg 1, 2628 CN Delft, The Netherlands

E-mail: w.h.vanderspoel@citg.tudelft.nl

ABSTRACT: An analytical model is presented that describes the water vapour permeability of a perforated foil in dependence of pinhole dimension, degree of perforation and water vapour permeability of the contacting media. A comparison of analytical solutions with numerical results indicates a good agreement when the degree of perforation is not too large. The differences are smaller than 15 % in case the ratio of pinhole surface area to total area is less than 5 %. Experimental data obtained by others are generally well described by the model, but differences are seen for foils attached to a solid material.

1 INTRODUCTION

In building practice, foils are used for waterproofing in the building phase, radiant barrier and vapour retarder. In many cases, except the latter, the foil should be open for water vapour transport to prevent condensation. This can be accomplished by perforation. Standardized tests are performed to measure the water vapour permeability of such foils. In these tests (e.g. DIN 53122) the foil forms the separation between two air volumes at equal and constant temperature but at different relative humidity. In practise, the foil is generally loosely attached to another material or rests e.g. on the roof boarding. The practical vapour permeability may therefore deviate from the measured value.

In this paper a simple analytical model is presented for the water vapour permeability of a perforated foil in dependence of perforation characteristics and the water vapour permeability of the contacting materials, and compared with measurement results. The influence of a small air layer between a less permeable material and the foil, air movement along and through the foil, water vapour permeation and capillary water transport in a contacting material are discussed.

2 ANALYTICAL MODEL

2.1 Transport equations

We limit the attention to isothermal diffusion of moisture in a material in the hygroscopic regime.

The moisture transfer may then be described by Fick's law:

$$\vec{j}_v = \frac{\delta}{\mu} \nabla p_v \quad (1)$$

with \vec{j}_v the water vapour flux density ($\text{kg m}^{-2} \text{s}^{-1}$), δ the water vapour permeability of air ($1,85 \cdot 10^{-10} \text{ s}$ at 20°C), μ the ratio of the water vapour resistance of the material and air (also known as the μ -value) and p_v the partial water vapour pressure (Pa). Although the μ -value may depend on the moisture content of a material, it is assumed to be constant. Using the equation of continuity, we find for stationary conditions:

$$\nabla \cdot \left(\frac{1}{\mu} \nabla p_v \right) = 0. \quad (2)$$

At an interface between two materials we have:

$$\vec{n} \cdot \vec{j}_{v,1} = \vec{n} \cdot \vec{j}_{v,2} \quad (3)$$

where \vec{n} is the normal vector and $\vec{j}_{v,1}$ and $\vec{j}_{v,2}$ are the water vapour flux density in the adjacent materials.

2.2 Problem domain

We limit the attention to a vapour-tight foil with perforations at regular positions. An example is shown in Figure 1 where the typical distance between the gaps is $2r_d$, which equals $(\sqrt{m})^{-1}$ with m the number of gaps per unit surface area. For other gap distributions, we define $r_d \equiv (2\sqrt{m})^{-1}$. The analytical model may not be applied if the distance between the gaps

varies too much. For instance, it is not supposed to be valid in case the distance between the rows in Figure 1 differs much from the distance between the columns.

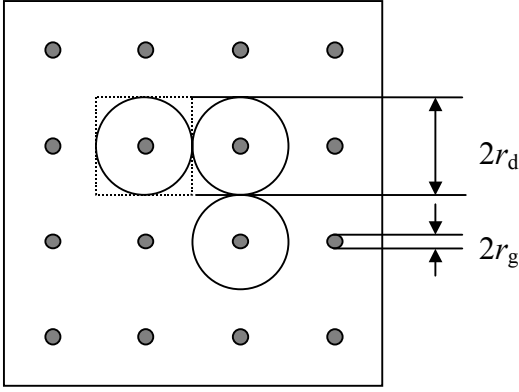


Figure 1: Example of a regular distribution of gaps in a foil. The distance between the gaps is $2r_d$ and the radius of each gap is r_g .

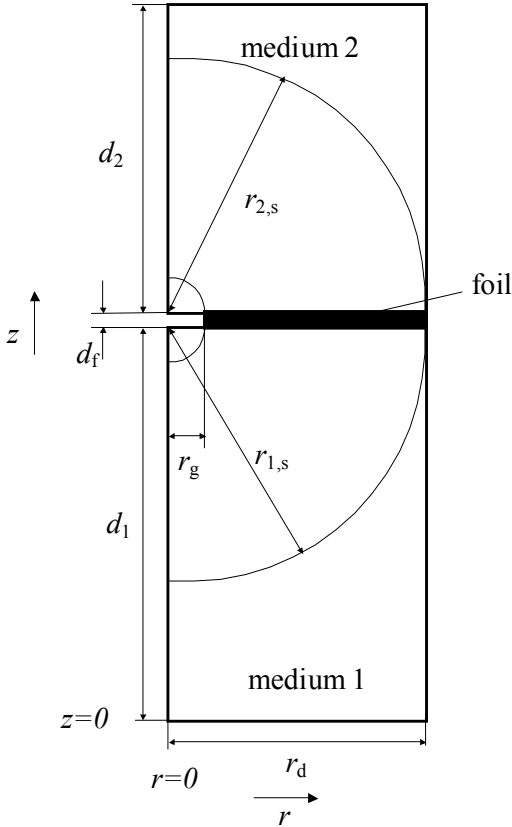


Figure 2: Schematic representation of the cylindrical problem domain. A vapour-tight foil with thickness d_f is situated between two media with thickness d_1 (lower side) and d_2 (upper side). The foil has a cylindrical gap with radius r_g . The problem domain radially extends to r_d , half of the typical gap-to-gap distance of the perforated foil.

For the model development, consider a hypothetical cylinder with radius r_d and its axis of symmetry perpendicular to the foil surface and through the midpoint of one of the gaps. We impose a cylindrical (r, z, φ) coordinate system, as shown in Figure 2 for relevant areas in the (r, z) -plane. The angle φ

may be ignored due to rotation symmetry. The boundaries in the z -direction correspond to the thickness of the (homogeneous) medium at a side of the foil, denoted as d_1 and d_2 for the lower and upper side, respectively. The thickness of the foil is d_f .

2.3 Boundary conditions

The problem domain is simplified by disregarding transport in the region between the dotted square and enclosed circle in Figure 1. As a result, the hypothetical boundary at $r = r_d$ in Figure 2 is supposed to be impermeable, i.e. $\partial p / \partial r = 0$ at $r = r_d$. The induced error by disregarding this region is small and will be discussed later. Furthermore, the partial water vapour pressure at the lower ($z = 0$) and upper domain boundary ($z = d_1 + d_f + d_2$) is supposed to be constant at $p_{v,1}$ and $p_{v,2}$, respectively.

2.4 Model description

In analogy with an electrical circuit with a series of ohmic resistors, the water vapour transport may be described by a series of regions each having a specific resistance. This resistance equals the ratio of the water-vapour pressure difference over the region and the corresponding vapour flux density and depends on the geometry and μ -value. Seven (homogeneous) regions are distinguished in Figure 2: three regions at each side of the foil and the gap itself. Because of symmetry, the lower side is only considered here.

At a larger distance ($> r_d$) from the gap, the transport in this first region is not much influenced by the foil. The vapour transfer is assumed to be one-dimensional (along z -axis) and may therefore be disregarded for evaluating the vapour resistance of the foil. The second region is considered to exist between two spheres with radius r_g and $r_{1,s}$ from the point $(0, d_1)$ situated just below the centre of a gap. We define $r_{1,s} \equiv r_d$ when $d_1 \geq r_d$, and $r_{1,s} \equiv d_1$ when $d_1 < r_d$. Assuming transport with spherical symmetry, the transport resistance is given by

$$R_{1,s} = \frac{\mu_1}{2\pi\delta} \left(\frac{1}{r_g} - \frac{1}{r_{1,s}} \right), \quad (4)$$

where μ_1 is the μ -value of medium 1. The third region lies between the spherical surface with radius r_g and the cylindrical surface of the gap opening ($0 < r < r_g, z = d_1$), where the transport develops from spherical to cylindrical symmetry. A simple analytical expression for the resistance can therefore not be given. Following the approach by Heiss (1954) and Lange et al. (2000), the resistance of this transition area is estimated at:

$$R_{1,t} = \frac{\mu_1}{3\pi\delta r_g}. \quad (5)$$

The two influencing regions at the upper side of the foil are modelled in a similar way. Finally, the resistance of the cylindrical gap itself is described by

$$R_g = \frac{\mu_g d_f}{\pi \delta r_g^2}, \quad (6)$$

where μ_g is the μ -value of the gap and d_f the thickness of the foil.

The total transport resistance R_{tot} of the region influenced by the foil is given by summation of five resistances. After some rearranging, we find

$$R_t = \frac{1}{\pi \delta} \left[\mu_1 \left(\frac{5}{6r_g} - \frac{1}{2r_{1,s}} \right) + \mu_2 \left(\frac{5}{6r_g} - \frac{1}{2r_{2,s}} \right) + \frac{\mu_g d_f}{r_g^2} \right]. \quad (7)$$

Effective μd -value of a perforated foil

For a simple one-dimensional or numerical calculation of water vapour transfer in a construction, it is practical to know the effective vapour resistance ($\mu_{\text{per}} d_f$) of a perforated foil. In principle, for one-dimensional transport we may write for the effective total resistance:

$$R_{\text{tot,eff}} = \frac{\mu_1 r_d + \mu_{\text{per}} d_f + \mu_2 r_d}{\pi \delta r_d^2}. \quad (8)$$

Equating with Equation (7) yields:

$$\mu_{\text{per}} d_f = r_d^2 \left[\mu_1 \left(\frac{5}{6r_g} - \frac{1}{2r_{1,s}} - \frac{r_{1,s}}{r_d^2} \right) + \mu_2 \left(\frac{5}{6r_g} - \frac{1}{2r_{2,s}} - \frac{r_{2,s}}{r_d^2} \right) + \frac{\mu_g d_f}{r_g^2} \right]. \quad (9)$$

Usually the gap-to-gap distance will be much larger than the gap radius, or $r_d \gg r_g$. If furthermore $d_1 \geq r_d$ and $d_2 \geq r_d$ (i.e. $r_{1,s} = r_{2,s} = r_d$) a good approximation is:

$$\mu_{\text{per}} d_f = \frac{r_d^2}{r_g} \left(\frac{5\mu_1}{6} + \frac{5\mu_2}{6} + \frac{\mu_g d_f}{r_g} \right). \quad (10)$$

where the third term at the right-hand side may be neglected for thin foils in proportion to the gap radius (and $\mu_g = 1$). The effective resistance of a thin foil is therefore 1) proportional to the sum of the μ -values of the media at both sides of the foil, 2) quadratically proportional to the gap-to-gap distance and 3) reversely proportional to the radius of the gaps. The first demonstrates that the apparent vapour resistance of a perforated foil can not be regarded independent of the vapour resistance of the contacting media. However, in many cases the third term at the right-hand side of Equation (10) should not be ignored.

3 COMPARISON WITH NUMERICAL CALCULATIONS

To gain some insight in the validity of the above idealised and simplified analytical model a comparison has been made with numerical calculations of diffusion through a pinhole for the geometry as shown in Figure 2. The comparison focuses on the effective resistance of the perforated foil and has been performed for several variants, involving the parameters μ_1 , μ_2 , d_1 , d_2 , r_g and r_d . The considered values are given in Table 1. The thickness of the foil is constant, $d_f = 0.3$ mm, and the gap is air-filled ($\mu_g = 1$). Due to symmetry only 126 of the 216 variants are principally different. The ratio of the numerically¹ and analytically calculated effective resistance $\mu_{\text{per}} d_f$ of these 126 variants as calculated with Equation (9) is shown in Figure 3, sorted by this ratio. It is seen that for a small group the numerical values are significantly larger than estimated with Equation (9). It appears that this group involves all cases for which both $r_g = 1$ mm and $r_d = 2$ mm. If we disregard this group, see inset in Figure 3, the differences between the analytical and numerical value are within 9 %.

Table 1. Values for μ_1 , μ_2 , d_1 , d_2 , r_g and r_d used in the calculations.

parameter	value #1	value #2	value #3	unit
μ_1	1	30		
μ_2	1	30		
d_1	2	8	32	mm
d_2	2	8	32	mm
r_g	0.25	1		mm
r_d	2	8	32	mm

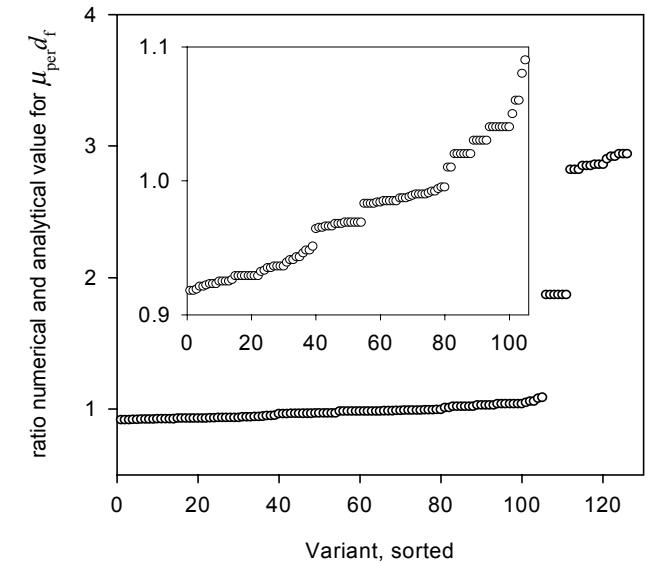


Figure 3. Ratio of numerically and analytically calculated effective diffusion resistance of perforated foil for the parameters shown in Table 1. Inset: enlargement of vertical axis for cases with $r_g = 1$ mm and $r_d = 2$ mm left out.

¹ Refinement of the numerical grid did not influence the results.

These results show that the analytical model agrees well with the numerical model, except when the gap diameter is not much smaller than the gap-to-gap distance. In that case, more or less linear transport occurs instead of spherical transport as assumed in the analytical model. These cases are characterised by a large degree of perforation n , defined as the ratio of gap area to total area:

$$n = \frac{\pi r_g^2}{(2r_d)^2}, \quad (11)$$

for a distribution as shown in Figure 1. For $r_g = 1$ mm and $r_d = 2$ mm the degree of perforation is 20 %. As the next largest degree of perforation in the previous set of calculations is 1.2 %, some additional calculations were performed with $0.012 < n < 0.2$. These results, together with the previous data, are shown in Figure 4 as a function of n . There is a clear correlation between the calculated ratio and the degree of perforation and it is seen that the differences are smaller than 15 % for $n < 5$ %. We may therefore conclude that Equation (9) is a good description for the effective μd -value of a perforated foil for a degree of perforation $< 5\%$.

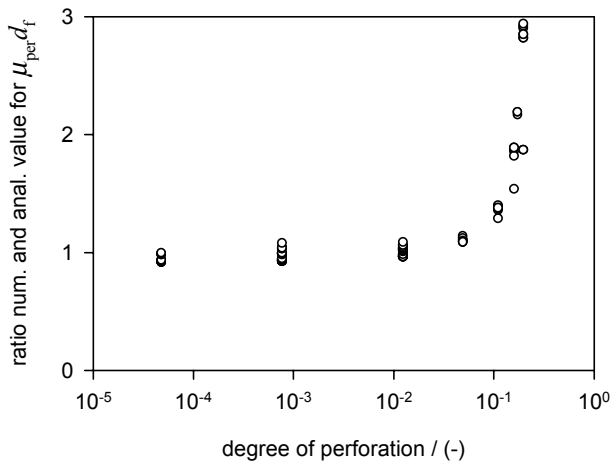


Figure 4: Ratio of numerically and analytically calculated effective diffusion resistance of a perforated foil as a function of the degree of perforation. Next to the variants shown in Figure 3, additional results are shown for which $0.012 < n < 0.2$.

4 COMPARISON WITH EXPERIMENTAL RESULTS

4.1 Measurements by Schüle & Reichardt

In this section we compare the analytical model with experimental results obtained by Schüle & Reichardt (1980) who measured the vapour flux through perforated metal plates for varying degree of perforation and gap diameter. Their 'first' set-up consisted of cups with silica gel, covered with either circular (190 mm diameter) or rectangular (110 x 230

230 mm²) 1 mm thick metal plates with 1, 5 or 9 gaps regularly distributed over the plate, with gap diameters of 1, 5, 10 or 20 mm, placed in a room at 23 °C and 50 % RH at practically still air (air velocity < 0.05 m s⁻¹). The vapour flux was derived from the rate of mass increase of the silica gel. The degree of perforation for reported data varies between 0.014 % and 10 %. In Figure 5 the modelled² (left axis) and experimental water vapour flux³ normalised to 1 Pa partial vapour pressure difference ($|p_{v,1} - p_{v,2}| = 1$ Pa) is plotted against each other (solid circles). For clarity, the relative difference (% , right axis) between these quantities is shown by open squares. The mean relative difference is -4 % with a maximum of 16 %. Although there is some tendency for a positive difference (model larger than experiment) for a smaller vapour flux density and vice versa, it may be concluded that the model, considering its accuracy of about 15 %, compares well with these experimental results.

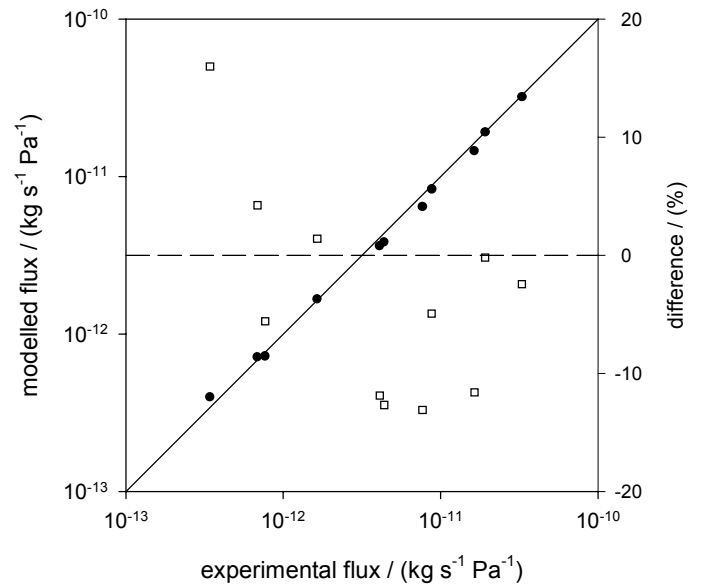


Figure 5. Left axis: analytically calculated water vapour flux plotted against the measured flux (solid circles). Right axis: relative difference (%) between the two values (open squares).

A second series of experiments focussed on the influence of the thickness of the metal plates d_f , i.e. on the gap depth. These measurements were done for 1, 2, 5 and 7 mm thick plates containing 1 gap with a diameter of 5 mm. The comparison with the modelled vapour flux is shown in Figure 6. Here a systematic difference between model and experiment is observed. The model starts to overestimate the measured values for larger plate thickness. For a 7 mm plate, the modelled value is a factor 1.5 higher than measured. This observation is quite opposite to expectations. As the vapour transport in the gap is linear one-dimensional and the diffusion resistance

² With $d_1 = d_2 = 40$ mm and $\mu_1 = \mu_2 = 1$.

³ Experimental uncertainty not reported.

of the gap (last term at the right-hand side of Equation (9)) starts to dominate for gap depths > 5 mm, the diffusion resistance is more well-defined from the modelling point of view. The cause of the difference is therefore not clear and probably not due to shortcomings of the model.

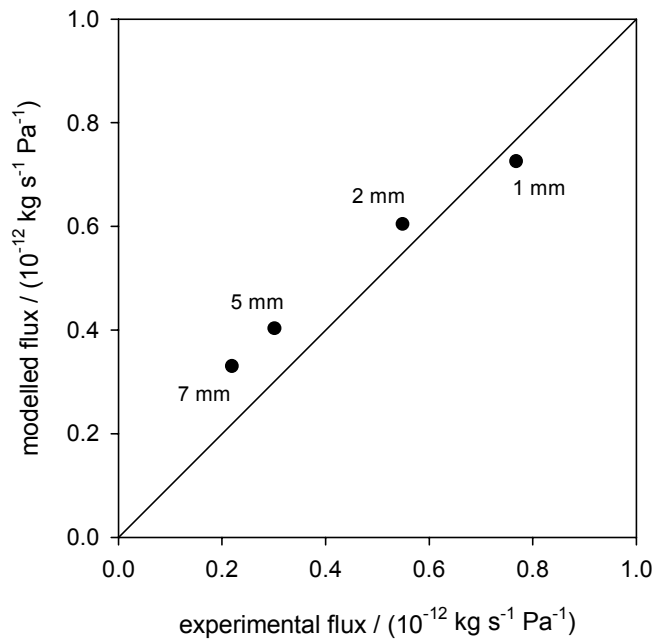


Figure 6. Analytically calculated water vapour flux plotted against the measured flux (solid circles) through a 5 mm diameter gap for different gap depth d_f , indicated in the graph.

A third series of experiments by Schüle and Reichardt concerned the effect of two isolating materials. Measurements were performed with 30 mm mineral wool (MW, $\mu = 2,6$) and 20 mm expanded polystyrene (PS, $\mu = 37$) attached to one side of a 1 mm thick perforated plate containing 5 gaps with 1, 5 and 10 mm gap diameter. In Figure 7 the modelled flux is plotted against the measured values for MW (solid circles) and PS (open circles). The differences between measurement and model are considerable for mineral wool ($< 50\%$) and large for polystyrene where differences of about a factor 4 to 5 are observed for all data points, the modelled values being lower than measured. This may partly be explained by a RH-dependent μ -value of the isolating material. A large part of the vapour resistance is determined by transport in the isolating material close to a gap where dry conditions (RH $< 20\%$) prevail, which may deviate from the humidity conditions at which the vapour resistance of the material is determined. The vapour resistance is known to decrease with decreasing relative humidity for some materials. Whether this holds for PS has not been verified. Another explanation might be the presence of a thin air-layer between the metal plate and isolating material. Numerical calculations indicate that a 0.3 mm air layer (and no leakage at the side of the cup) rises the vapour flux by a factor 3 to 5. Unfortunately, these suppositions can not be verified.

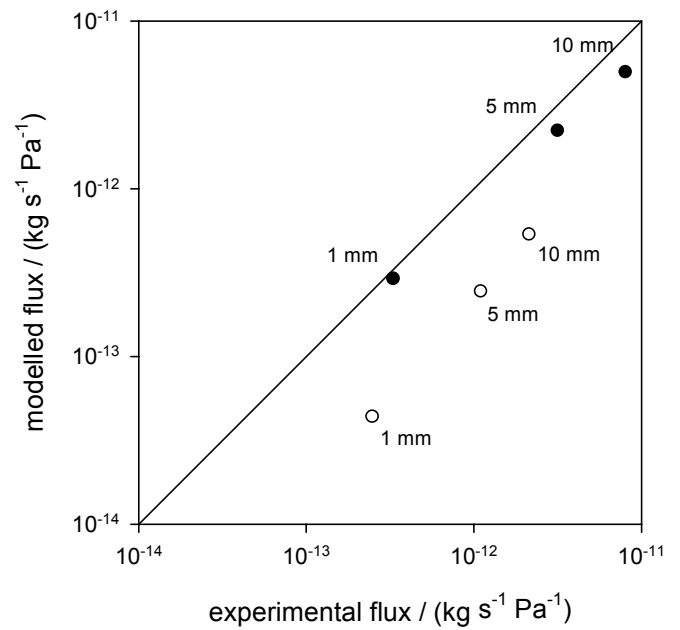


Figure 7. Analytically calculated water vapour flux plotted against the measured flux for a configuration with 30 mm mineral wool (solid circles) and 20 mm expanded polystyrene (open circles) attached to a perforated metal plate with 5 gaps for different gap diameter r_g , indicated in the graph.

4.2 Perforated foils

The dimensional parameters r_g , r_d and d_f of three commercially available perforated foils have been measured and used in the analytical model to calculate the water vapour permeability (at $\Delta p_v = 2400$ Pa). This predicted value is compared with the measured value cited by the representative. The characteristics of the polyethylene foils and the predicted and measured water vapour permeability are given in Table 2. The prediction significantly underestimates the measured value for foil #1 whereas there is a reasonable correspondence for foil #2 and a slight overestimation for foil #3. The uncertainty in the predicted value for foil #2 is however large due to a strong deformation of the polyethylene near the perforations which results in tortuous gaps that are much longer than the foil itself. This impedes an accurate measurement. To a lesser extent this also accounts for foil #3, which may explain the overestimation. The underestimation for foil #1 may be caused by vapour transport through the foil material.

Table 2. Measured foil parameters and predicted water vapour permeability of three commercial perforated foils. Uncertainty in predicted value reflects uncertainty in gap radius and length.

Foil	r_g μm	r_d mm	d_f μm	measured permeab. ($\text{g m}^{-2} 24\text{h}^{-1}$)	predicted permeab. ($\text{g m}^{-2} 24\text{h}^{-1}$)
Foil #1	27	5.3*	95	25	7 ± 2
Foil #2	175§	4.3#	500§	100	80 ± 25
Foil #3	67	1.96§	150	140	170 ± 15

* 9000 gaps m^{-2} , # 13800 gaps m^{-2} , § 83000 gaps m^{-2}
§ rough estimates, foil thickness is 100 μm

5 DISCUSSION

To what extent the simplifications in the analytical (and numerical) model are permissible for application under practical conditions, is discussed.

Idealisation of the problem domain

Both the analytical and the numerical model assume an impermeable boundary at the cylindrical wall $r = r_d$. This procedure disregards transport in the region between the (dotted) square and the inner circle. The induced error is however small for a perforation degree $< 5\%$. Instead of r_d as typical radius, we could have chosen r'_d corresponding to a circle with surface area equal to the dotted square, i.e. $r'_d \approx 1.13 r_d$. For a perforation degree $n = 5\%$ the effect on the total diffusion resistance is only 2% .

The analytical model also disregards the transport resistance of the area between the surface $z = d_1 - r_{1,s}$ and the halve sphere with radius $r_{1,s}$, see Figure 2 (mutatis mutandis for the other side of the foil). In this area the diffusive transport switches over from linear to spherical symmetry. Since this transition area is correctly described by the numerical model, there is no effect on the data shown in Figure 3. It may however explain a calculated ratio < 1 for a large part of the data in this figure.

Vapour permeability of the foil material

In practice, synthetic foils are to some extent permeable to water vapour whereas Equation (9) is only applicable if the vapour flux through the foil material is much smaller than the flux through the gap. For a first-order estimate of the ratio of these fluxes we assume two independent parallel transport paths through the foil material and the gap. If we impose the Dirichlet boundary conditions at the foil surface, the total effective μ -value of a perforated foil is approximated by

$$\mu_{\text{eff}} = \left(\frac{1}{\mu_{\text{per}}} + \frac{1}{\mu_f} \right)^{-1}, \quad (12)$$

where μ_f is the μ -value of the foil material. This is a lower-bound estimate of the effective resistance, i.e. the true flux through the foil material will be somewhat lower.

Air flow through the foil

The model has been derived for stagnant air. But, air will flow through the gaps in response to air-pressure differences over the foil. Typical air pressure difference found in practise due to wind and thermal buoyancy are of the order of $1 - 10$ Pa. To estimate the effect of an air flow through a perforated foil, we consider the Peclet number of the flow, characterising whether the water vapour trans-

port is diffusion dominated ($Pe < 1$) or advection dominated ($Pe > 1$), defined as

$$Pe = \frac{v_{\text{char}} d_{\text{char}} \mu}{D_0} \quad (13)$$

where v_{char} and d_{char} are a characteristic velocity and distance of the flow and D_0 the diffusion coefficient of water vapour in air (approx. $2.5 \cdot 10^{-5} \text{ m}^2 \text{ s}^{-1}$). As yet, the foil is thought to be situated between air layers, i.e. $\mu = 1$;

Consider again Figure 2. As a result of an air-pressure difference Δp_a between the surfaces ($z = 0$) and ($z = d_1 + d_f + d_2$), a flow rate Q is induced through the gap. The air flow through the foil can either be 'creeping' (viscous) or turbulent. In case of creeping flow, we have to a very good approximation (Dagan et al., 1982; Sisavath et al., 2002):

$$Q = \frac{\Delta p_a}{\left(\frac{3\mu_v}{r_g^3} + \frac{8d_f\mu_v}{\pi r_g^4} \right)}, \quad (14)$$

where μ_v the viscosity of air ($1.8 \cdot 10^{-5} \text{ Pa s}$). Viscous forces dominate for Reynolds number < 1 , defined as

$$Re = \frac{\rho v_{\text{char}} d_{\text{char}}}{\mu_v}, \quad (15)$$

where ρ is the air density ($\approx 1.2 \text{ kg m}^{-3}$). Combining with Equation (13) gives

$$Re = \frac{\rho D_0}{\mu_v} Pe = Sc^{-1} Pe, \quad (16)$$

where Sc is the Schmidt number (0.6 for air at 20°C) which shows that diffusion will dominate the transport of water vapour for creeping flow conditions. It is however not so easy to specify the characteristic velocity and distance for the problem at hand. At first instance, we might take the velocity in the gap and gap radius. But, since the transport process is largely governed by the converging and diverging flow field at some distance from the gap, we take, as a trade-off, the flow velocity at the spherical surface with 'characteristic' radius $2r_g$ from a gap. The average flow velocity at this sphere is

$$v_{\text{char}} = \frac{Q}{2\pi(2r_g)^2}, \quad (17)$$

and therefore, using Equation (14):

$$Re = \frac{\rho v_{\text{char}} d_{\text{char}}}{\mu_v} = \frac{\rho r_g^2 \Delta p_a}{4\mu_v^2 (3\pi + 8(d_f/r_g))}. \quad (18)$$

For example, viscous dissipation and therefore vapour diffusion will dominate at 10 Pa pressure difference for gap radii smaller than $60 \mu\text{m}$ for a foil of thickness $d_f = 100 \mu\text{m}$. For these parameters and e.g.

a degree of perforation of 0.01 %, the flow rate through a unit area of perforated foil is 0.2 L s^{-1} , a reasonable value from a practical point of view. For larger gap radii convection may dominate depending on the pressure difference over the foil.

For turbulent flow we may use the well-known orifice equation as an approximation ($r_d \gg r_g$) to calculate the flow rate:

$$Q = C_d \pi r_g^2 \sqrt{\frac{2\Delta p}{\rho}} \quad (19)$$

where C_d is the discharge coefficient which is approximately 0.6 for high Reynolds number (Bird et al., 1960). As the vapour transport is dominated by convection in this flow regime, the vapour flux J_v (kg s^{-1}) through the gap may then be approximated by:

$$J_v = Q \frac{p_v}{R_w T} \quad (20)$$

where p_v is the partial water vapour pressure at the high air-pressure side of the foil, R_w the gas constant of water ($462 \text{ J kg}^{-1} \text{ K}^{-1}$) and T the temperature.

The above equations do not hold for foils attached (at one side) to an air-permeable material. If we assume that Darcy's law holds for air-flow in such a medium:

$$\vec{q}_a = \frac{K}{\mu_v} \nabla p_a \quad (21)$$

where \vec{q}_a is the air flux density ($\text{m}^3 \text{ m}^{-2} \text{ s}^{-1}$) and K (m^2) the permeability of the medium, there is a mathematical correspondence with Equation (1). If we further assume that the resistance to air flow is completely determined by the material, we have for the air-flow rate through the gap, following Equation (10) for $r_d \gg r_g$ (and $d_1 \geq r_d$; $d_2 \geq r_d$):

$$q = \frac{6K r_g \Delta p_a}{5\mu_v} \quad (22)$$

so, using Equations (13) and (17), the Peclet number is

$$\text{Pe} = \frac{3\mu K \Delta p_a}{10\pi\mu_v D_0} \quad (23)$$

For an extremely open medium (e.g. coarse sand) $K = 5 \cdot 10^{-11} \text{ m}^2$ and $\mu \approx 2$, we find $\text{Pe} = 0.2$ at 10 Pa pressure difference. As for other denser materials, the product μK usually decreases, it is concluded that diffusion will nearly always dominate the vapour transport mechanism for foils attached to a solid material.

Air flow along the foil

For air flow along the foil we use the lateral velocity u_x at a distance $2r_g$ from the foil as the charac-

teristic velocity. This velocity however strongly depends on the circumstances. For a foil exposed to the climate, wind gusts may locally impose large velocities in absence of a developed boundary layer. On the other hand, in practise perforated foils are usually installed in a cavity and are thus sheltered from the wind. To obtain some quantitative idea, consider one-dimensional laminar flow in a d m wide cavity for which the lateral flow velocity u_x is described by

$$u_x = 4u_{\max} \left(\frac{y}{d} - \left(\frac{y}{d} \right)^2 \right); \quad y \leq \frac{1}{2}d, \quad (24)$$

where y is the perpendicular distance from one of the sides and u_{\max} is the maximum velocity, at $y = d/2$. At a distance $y = 2r_g$ and $r_g \ll d$, the Peclet number is

$$\text{Pe} = \frac{16u_{\max} r_g^2}{dD_0} \quad (25)$$

For $d = 0.02 \text{ m}$ and $u_{\max} = 0.1 \text{ m s}^{-1}$, we find $\text{Pe} = 1$ for $r_g = 0.56 \text{ mm}$. This indicates that diffusion will dominate in most circumstances because the gap radius is usually smaller and higher velocities are not expected to occur frequently. Exceptions may concern cavities that are well ventilated with outdoor air. Note that air flow along an attached foil will normally have no influence on the vapour flux as the largest diffusion resistance lies in the solid material.

Connection with the substrate

In practise perforated foils are often loosely attached (stapled) to a substrate material, which results in a small air layer (plenum) between the foil and the material. Such an air layer has a strong effect on the effective vapour resistance of the foil. Numerical calculations indicate that for a 1 mm air layer between a foil and a material with $\mu = 30$, the vapour resistance is decreased by about an order of magnitude. Evidently, the analytical model can not be used for such configurations. As moreover in practise the air-layer thickness will vary over the foil, the description of the vapour transfer becomes very difficult and three-dimensional (a problem that does not arise for non-perforated foils). An accurate description of the vapour transfer through a perforated foil can therefore only be given for a perfect connection to a substrate or if the air layer thickness is at least about the size of the gap-to-gap distance.

Water transport in the substrate

The model assumes that the moisture transport in the substrate is dominated by vapour transfer, i.e. that the moisture content, for a porous material, is below the critical value. If the moisture content is above that value, the moisture transfer is dominated by capillary water transport which is normally much faster than vapour transfer. In that case, an effective

vapour resistance of the foil may be derived based on the assumption that the moisture transport in the substrate does not contribute to the total transport resistance. It is then allowed to use Equation (9) with the μ -value of the substrate set to zero.

It should however be remarked that this simple view may not reflect reality. As the material may dry quickly near a gap (the vapour flux density is locally higher than for an uncovered surface), it is conceivable that the capillary transport is not fast enough to keep up with the transfer rate. As a result, a new equilibrium may set in where the moisture content becomes sub critical near the gap. To what extent this happens depends on the moisture transport characteristics of the porous material. In any case, capillary water transport will lower the effective resistance of the foil.

6 CONCLUSIONS

A simple analytical model has been developed that predicts the water vapour permeability of a perforated foil in dependence of the gap radius, gap-to-gap distance, foil thickness and the vapour resistance of the substrate material (if present). According to this model, the effective resistance of a thin perforated foil is, under most circumstances, linearly proportional to the μ -value of the substrate material(s), quadratically proportional with the gap-to-gap distance and reversely proportional to the radius of the gaps. A comparison with more precise numerical calculations of diffusive water vapour transport shows that the model predicts the permeability within 15 % if less than 5 % of the foil surface is perforated.

A similar agreement is observed in comparison with measurement results obtained by others for water vapour transport through thin perforated metal plates. Somewhat larger deviations are observed for measurements with thicker perforated plates but this is probably not due to weaknesses of the model. Very large differences of about a factor 5 are however seen for perforated plates attached to a material with a μ -value of 37. It is speculated that this might be caused by a thin air-layer between the plate and the material. Furthermore, the model reasonably predicts the water vapour permeability of one commercially available perforated polyethylene foil but underestimates the permeability for another by a factor 3. This comparison should actually include more foils to obtain a better insight.

There are circumstances in practise that violate the model assumption of pure diffusive transport. A key factor in this context concerns the air-flow velocity through and along the foil. Although diffusive transport will dominate in most cases, there are some configurations for which convective transport will

have an influence depending on the climate conditions. Air flow along a perforated foil will always enhance the vapour transport through the foil, whereas air flow through the foil may also decrease the vapour flow depending on the flow direction.

Another outcome of the model is the strong influence of the vapour resistance of the substrate on the effective vapour permeability of the foil. As the water vapour resistance of a perforated foil is usually measured with air at both sides of the foil, it is not allowed to use this value for calculating the vapour resistance of e.g. a wall or roof assembly if the foil is tightly attached to a substrate.

REFERENCES

- Bird, R.B., Stewart, W.E. & Lightfoot, E.N. 1960. Transport Phenomena. John Wiley & Sons: New York.
- Dagan, Z., Weinbaum, S & Pfeffer, R. 1982. An infinite-series solution for the creeping motion through an orifice of finite length. *J. Fluid Mech.* 115: 505-523.
- Heiss, R. 1954. Verpackung feuchtigkeitsempfindlicher Lebensmittel. Springer: Berlin.
- Lange, J., Büsing, B., Hertlein, J., and Hediger, S. 2000. Water Vapour Transport through Large Defects in Flexible Packaging: Modeling, Gravimetric Measurement and Magnetic Resonance Imaging. *Packag. Technol. Sci.* 13: 139-147.
- Schüle, W. & Reichardt, I. 1980. Wasserdampfdurchgang durch Öffnungen. *Zeitschrift für Wärmeschutz, Kälteschutz, Brandschutz.* WKS-B-Sonderausgabe August 1980: 12-16.
- Sisavath, S., Jing, X., Pain, C.C, Zimmerman, R.W. 2002. Creeping Flow Through an Axisymmetric Sudden Contraction of Expansion. *J. Fluids Eng.* 124: 273-278.

